Classical Collisional Diffusion in the Annular Penning Trap

Qudsia Quraishi,* Scott Robertson,* and Bob Walch†

*Department of Physics, University of Colorado, Boulder, Colorado 80309-0390
†Department of Physics, University of Northern Colorado, Greeley, Colorado 80639

Abstract. Transport of particles and energy by cross-field diffusion has been studied in the annular Penning trap in which a nonneutral plasma of electrons is contained between concentric cylinders. At densities sufficiently low ($<10^5$ cm^{-3}) to suppress mobility transport arising from the space charge electric field, the dominant source of transport is diffusion from collisions of electrons with added helium gas. The particle diffusivity, when corrected for asymmetry transport, is observed to scale linearly with collision frequency and inversely with the square of the axial magnetic field. Measurements of the electron energy distribution as a function of time show an initial mean energy of 0.3 eV which decreases with time as a result of diffusion cooling.

INTRODUCTION

The classical diffusivity coefficient of electrons perpendicular to a magnetic field can be written as $D_\perp = \nu_c \, r_L^2$, where ν_c is the frequency of electron collisions with another species and r_L is the thermal Larmor radius. There is limited experimental data that supports this equation. In charge neutral plasmas, cross-field diffusion of electrons and ions occurs at the ambipolar rate. Electrostatic turbulence driven by currents or density gradients often causes additional transport that masks the classical transport. Current driven turbulence is absent in the Q-machine and in afterglows and in these plasmas demonstration of proper scaling of ambipolar diffusion with magnetic field and with collision frequency has been possible.[1,2] In the Malmberg-Penning trap, transport of electrons has been measured arising from collisions with a background gas.[3,4] In this trap, the space charge electric field of the electrons usually results in transport by mobility being greater than that by diffusion. In this work, we examine diffusion of electrons in an annular version of the Malmberg-Penning trap[5] in which electrons are confined between concentric cylinders at ground potential. The electrons are confined radially by an axial magnetic field and axially by negative potentials applied to grids at the ends. At sufficiently low density, the mobility transport from the space charge electric field is much smaller than the diffusive transport. We demonstrate for a wide range of magnetic fields and collision frequencies that the measured diffusivity, when

CP606, *Non-Neutral Plasma Physics IV*, edited by F. Anderegg et al.

corrected for additional transport from trap asymmetry, has the expected classical scaling with collision frequency and magnetic field. The data also show that the mean electron energy falls with time as a consequence of diffusion cooling.

Theoretical treatments of transport beginning with the fluid equations in cylindrical geometry give a radial particle flux

$$\Gamma = -D_\perp \frac{dn}{dr} + n\,\mu_\perp E_r, \tag{1}$$

where,

$$D_\perp = \nu_c\, m\, T/q^2 B_z^2 = \nu_c\, r_L^2, \tag{2}$$

is the perpendicular diffusion coefficient,

$$\mu_\perp = m\nu_c / qB_z^2, \tag{3}$$

is the perpendicular mobility coefficient, n is the electron density, m is the electron mass, ν_c is the electron-neutral collision frequency, T is the electron temperature in energy units, r is the radial cylindrical coordinate, q is the negative electron charge, E_r is the radial electric field, and B_z is the axial magnetic field. For collisions of electrons with neutral gas, the collision frequency does not vary spatially and the diffusion equation has the same form as the equation for heat conduction. For concentric cylinders of radii r_o and $2r_o$ and for a constant diffusivity, the e-folding time for the lowest order mode[6] is $\tau_D = 0.1025\ r_o^2 / D_\perp$. This decay time is very nearly that for parallel planes of separation r_o, which is $(r_o/\pi)^2/D_\perp$. The temperature dependent diffusivity $D_\perp$ decreases with time as a consequence of the diffusion cooling, thus the exponential dependence of the decay time is an approximation.

For measurement of diffusion alone, electric fields must be kept sufficiently small for transport by mobility to be much less than that by diffusion. With the concentric cylinders kept at ground potential, a residual electric field arises from the space charge of the electrons. The ratio of the mobility flux to the diffusive flux can be found approximately by modeling the cylinders as parallel plates. In this case, the lowest order solution to the diffusion equation has a density which varies with distance as $n_0 \sin(\pi x/L)$ where x is the coordinate, L is the plate separation, and n_o is the central density. This gives, from Poisson's equation, a sinusoidal potential distribution with a peak value $\phi_o = n_o\, q\, L^2 / \varepsilon_o \pi^2$ and a cosinusoidal electric field with amplitude $E_o = n_o\, |q|\, L / \varepsilon_o \pi$. The ratio of the mobility flux at the boundary Γ_m to the diffusive flux at the boundary Γ_D is approximately

$$\frac{\Gamma_m}{\Gamma_D} = \frac{n_o \mu_\perp E_o}{D_\perp \dfrac{dn}{dx}} = \left(\frac{L}{\pi\lambda_D}\right)^2, \tag{4}$$

where λ_D is the Debye length. The mobility flux at the wall is overestimated by $n_o \mu_\perp E_o$ because the density at the wall is zero rather than n_o. Thus we can ensure that the diffusive flux is dominant by reducing the density such that $\lambda_D > L/\pi$. For concentric cylinders of separation r_o, the plate separation L is replaced by r_o. A similar inequality applies to transport in the usual Malmberg-Penning trap.[4]

THE APPARATUS

The annular Penning trap used for this study has larger dimensions and a greater magnetic field than the trap described previously.[5] The new trap, Fig. 1, is designed to have the maximum plasma volume that will fit inside a preexisting vacuum chamber and water-cooled coil set. There are eight pancake-like coils with a bore of 30 cm which are spaced to create a field which varies < 1% within the trapping volume. The vacuum is created by a 20-cm diffusion pump and the base pressure is ~10^{-7} Torr. The pressure of helium is set by a precision leak valve and is measured by an ionization gauge tube located 1.2 m above the experiment. The gauge is calibrated for N_2 and the reading is divided by 0.2 to correct for the differing response to He.

The trapping volume is between concentric cylinders of electropolished stainless steel 61 cm in length. The inner cylinder has an outer radius of r_o = 38.1 mm and the outer cylinder has in inner radius of 74.2 mm giving an aspect ratio of 1.95 and a trapping volume of 7.7 liters. Adjacent to the ends of the cylinders are annular grids with 85% transparency that are held at −24 V to confine the electrons. Experiments consist of repeated fill, hold, and dump cycles controlled by a computer interface. Data are acquired at intervals of 10 or 20 μs, which is much shorter than the experimental time scales of 10–300 ms.

The trap is filled with secondary electrons from helium that are created within the trap by a stream of primary electrons from a filament at one end. The filament is oriented radially and spans the distance from the inner cylinder to the outer cylinder. The filament is biased to −140 V for a few milliseconds to load the trap. The background gas is helium because low energy collisions of electrons with helium are elastic and the collision cross section for momentum transfer varies slowly with energy.[7,8] The energies of the confined electrons are usually below 1 eV and the cross section rises about 20% between 0 eV and 1 eV. The electron-neutral collision frequency is $\nu_c = n_{He}\, \sigma(\mathrm{v})\, \mathrm{v}$, where v is the electron velocity, $\sigma(\mathrm{v})$ is the collision cross section, and n_{He} is the helium density, and is shown as a function of electron energy in Fig. 2a. The relationship between the filling density, helium pressure and the current of primaries was investigated in the smaller trap.[9]

The electron density profile is measured by removing one grid potential to dump the confined charge onto a set of five concentric annular rings. A grounded grid adjacent to the annuli reduces electrostatic pickup from the switched grid. Active integrators measure the collected charge. The charge is corrected for the absorption by the two meshes and the density is calculated by assuming that it is uniform along the length of the cylinders.

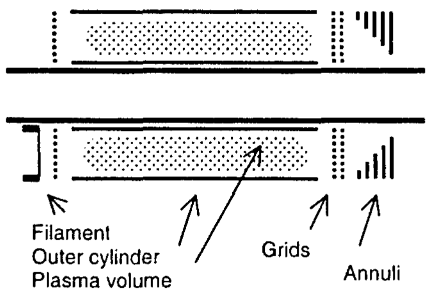

FIGURE 1. Schematic diagram of the annular Penning trap (not to scale).

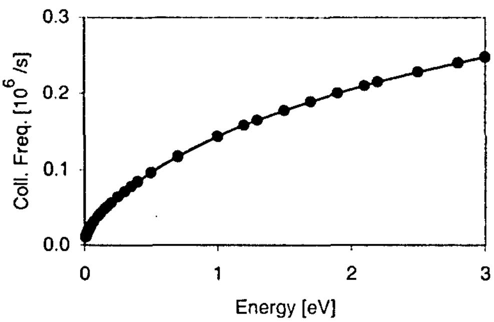

A)

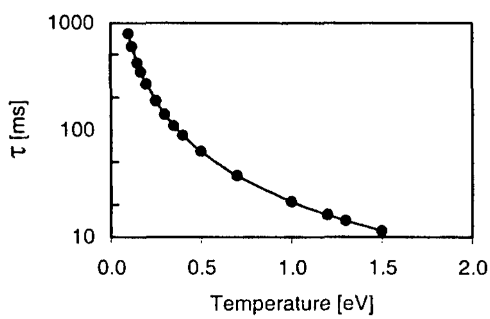

B)

FIGURE 2. (A) The collision frequency from the tabulated cross sections in reference [7] as a function of energy at a helium pressure of 1 mTorr. (B) The calculated diffusive decay constant τ_D from Eq. (2) as a function of temperature for B_z = 35 mT and a pressure of 1 mTorr.

The electron temperature is determined by lowering the potential barrier so that electrons are dumped onto the annuli in a time of order one millisecond. The current collected at an annulus at each instant is determined by the number of electrons just able to cross the falling potential barrier and is thus proportional to the distribution function.[10] The confining voltage V is switched from -24 V to -5 V and then is ramped linearly through zero at a rate of 1 V/ms. With finite electron density, there is a negative space charge potential with a peak value ϕ_o midway between the cylinders. Electrons with kinetic energy at the midplane greater than $q(V-\phi_o)$ are those able to pass the barrier. Electrons have a large number of collisions (~400 at 0.1 eV) during the sweeping of the analyzer voltage, thus the losses from the trap include all the particles with total kinetic energy greater than $q(V-\phi_o)$. This principle of operation is different from that of an analyzer in a collisionless plasma for which the detected particles are those with parallel energy greater than $q(V-\phi_o)$. At the low densities used in these experiments, $\phi_o < 0.1$ V.

EXPERIMENTS

Experiments are performed using repeated fill, hold and dump cycles shown in Fig. 3. The overlapping traces are from the charge integrator connected to the middle annulus. The axial field is 35 mT and the pressure is 0.5 mTorr. The trap is filled by biasing the filament negatively for 6 ms. During this interval, primary electrons strike the annulus and create the charge pedestal seen at early times. The confined electrons are dumped onto the annulus after a 20 ms holding period that is increased in increments of 7 ms. The filament heating is adjusted so that at the first dump time the charge collected is approximately 18 pC, which corresponds to an initial density of 7×10^4 cm^{-3}. This gives a plasma frequency of 1.5×10^7 s^{-1}, which is very much less than the cyclotron frequency of 6×10^9 s^{-1}.

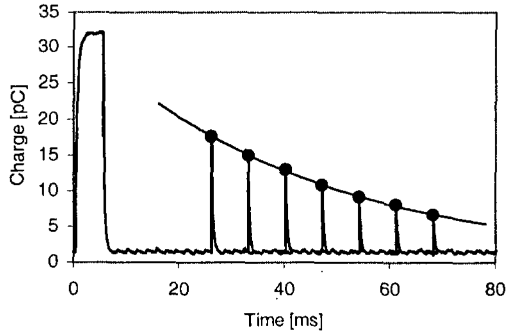

FIGURE 3. Oscillograms showing operation of the experiment. The signals show the charge dumped on the middle annulus for seven fill, hold and dump cycles. The curve passing through the peaks is a fitted exponential function determined by the least-squares method. For these data, B_z = 35 mT and the pressure is 0.5 mTorr.

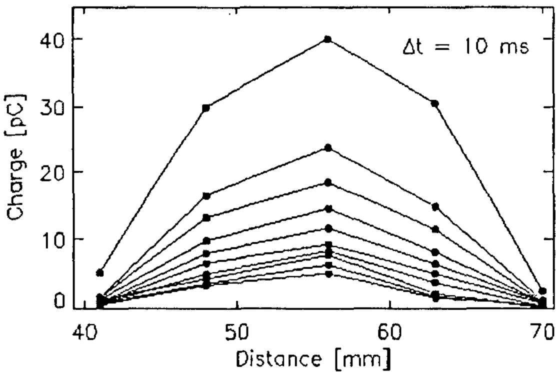

FIGURE 4. A plot of the radial distribution of density as a function of time. These data are for an axial field of 35 mT and a pressure of 0.5 mTorr. The interval between profile measurements is 10 ms.

The effect of mobility transport arising from the space charge electric field was quantified by taking additional data with initial charges of 36 and 54 pC. The e-folding times were observed to fall 10% with each 18 pC increase. Thus the measured e-folding times with 18 pC of initial charge are approximately 10% lower than the value obtained by extrapolating the data to zero charge.

Density profiles are obtained as a function of time by recording the charge dumped onto each of the five annuli at successively later times. A typical set of density profiles is shown in Fig. 4 for the same conditions as in Fig. 3. The profile is peaked in the center and decays self-similarly indicating that the lowest order mode of the diffusion equation is dominant.

The distribution function measured by lowering the grid potential is shown in Fig. 5 for standard conditions, 35 mT and 0.5 mTorr, and for hold times of 9, 10, 12, and 16 ms. These data were taken with 9 pC of initial charge for which $\phi_0 < 0.05$ V and thus the data are not corrected for the effect of space charge potential. The nonzero values for f(E) at negative energies are due to the finite response time of the electronics. The point at which the signal has fallen to half its peak value after the zero is passed, –0.05 V, is therefore an approximate measure of the resolution of the energy analyzer. The mean energy calculated from the measured distribution function is 0.3 eV at the first dump time. The initial mean energy varies weakly with magnetic field and filling pressure. The mean energy, when used as the temperature, gives a Debye length of 15 mm and a thermal Larmor radius of 0.04 mm at 35 mT. The inequality to make the mobility transport small, $\lambda_D > r_0 / \pi = 12$ mm, indicated by Eq. (4), is barely satisfied. However, comparisons of data with different filling densities show that the additional transport from mobility is indeed small thus indicating that the inequality is too stringent.

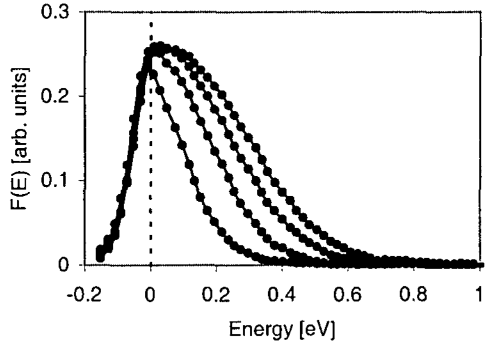

FIGURE 5. The distribution function f(E) at the middle annulus for hold times of 9, 10, 12, and 16 ms, an axial field of 35 mT and a pressure of 0.5 mTorr. The distribution becomes narrower with time.

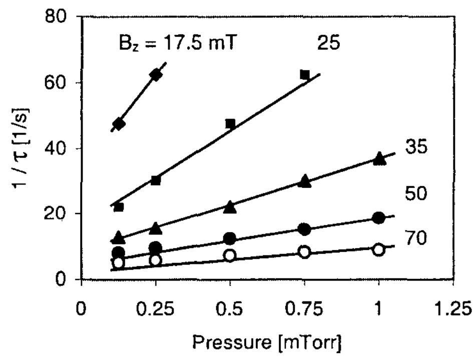

FIGURE 6. Dependence of the fitted decay constant upon the pressure of helium at magnetic fields of 17.5, 25, 35, 50, and 70 mT.

The dependence of the decay constant ($1/\tau_D$) upon the pressure of helium is shown in Fig. 6 for five values of magnetic field and five values of pressure. A linear dependence upon pressure is expected from the linear dependence of diffusivity upon collision frequency. Linear regressions made to the data do not extrapolate to zero diffusivity at zero pressure indicating an additional mechanism for loss. Experiments in the Malmberg-Penning trap have shown the existence of transport arising from trap asymmetries[11,12,13] which becomes evident at low pressure. The asymmetries may have their origin in the construction of the trap, misalignment of the trap with the magnetic field, or from electric fields arising from contact potentials. There is a range of parameters in the Malmberg-Penning trap for which the asymmetry transport scales inversely with the square of B_z. In Fig. 6, the solid line at 35 mT is a linear regression to the data. The lines at other magnetic fields are this regression scaled inversely with the square of B_z. These lines are good fits to the data and indicate that both the collisional transport and asymmetry transport have approximately the same inverse-square scaling with magnetic field. The accessible region of parameter space is limited to $B_z < 70$ mT by the magnetic field power supply and to pressures of ≤ 1 mTorr by the vacuum gauge. Data are also limited to decay times longer than 10 ms as a result of time constants associated with the diagnostic system. This prevents acquisition of data with both the highest pressures and lowest magnetic fields.

The four data points in Fig. 6 at the highest two fields and lowest two pressures lie slightly above the scaled regression. The longest confinement times cause the temperature to fall more slowly which increases the decay constant. This data could be scaled in a way that removes the temperature dependence. However, this region of parameter space is dominated by asymmetry transport and the temperature dependence of this transport in the annular trap has not been established.

The initial temperature value of 0.30 eV gives a calculated e-folding time of 140 ms (Fig. 2b) at a pressure of 1 mTorr and a magnetic field of 35 mT. The corresponding decay constant is 7 s^{-1}. The fitted decay constant at these conditions from Fig. 6 is 38 s^{-1}. The data at low pressure indicates that 8 s^{-1} of this is due to asymmetry transport. Thus that part of the decay constant from collisions is 30 s^{-1}, which is approximately a factor of 3.7 greater than that calculated from the collision cross section. It is inappropriate, however, to expect close agreement between the fitted e-folding times and τ_D from the fluid approach with constant $D_\perp$ because f(E) is not Maxwellian and the falling mean electron energy results in a time dependence which is not exponential.

SUMMARY AND CONCLUSION

An annular Penning trap confining a nonneutral low density plasma of electrons has been used to measure the diffusive cross-field transport from collisions of the electrons with helium gas. The measured decay times are reduced by about 10% by the additional transport from mobility driven by the space charge electric field. There is also transport from asymmetry that is found by extrapolation of the data to zero helium density. This contribution to transport is then subtracted from the data to obtain that part of the decay constant due to collisions. The corrected decay constants scale classically, i.e., linearly with the helium density and as the square of the magnetic field. The falling electron temperature results in a time dependent diffusivity. Precise comparisons between measured and calculated decay times will require numerical solutions to the equations for both particle and thermal transport.

ACKNOWLEDGMENTS

The authors acknowledge the assistance of John Klein and Matt Triplett in the development of the apparatus and diagnostic tools.

REFERENCES

[1] N. D'Angelo and N. Rynn, *Phys. Fluids* **4**, 1303 (1961).
[2] A. I. Anisimov, N. I. Vinogradov, V. E. Golant, and B. P. Konstantinov, *Sov. Phys. – Tech. Phys.* **7**, 884 (1963).
[3] J. S. DeGrassie and J. H. Malmberg, *Phys. Fluids* **23**, 63 (1980).
[4] M. H. Douglas and T. M. O'Neil, *Phys. Fluids* **21**, 920 (1978).
[5] S. Robertson and B. Walch, *Rev. Sci. Instrum.* **70**, 2993 (1999).
[6] H. S. Carslaw and J. C. Jaeger, *Conduction of Heat in Solids* (Oxford University Press, London, 1959), second edition, Chapter 7.10.
[7] R. W. Crompton, M. T. Elford, and R. L. Jory, *Aust. J. Phys.* **20**, 369 (1967).
[8] R. W. Crompton, M. T. Elford, and A. G. Robertson, *Aust. J. Phys.* **23**, 667 (1970).
[9] B. Walch and S. Robertson, *Phys. Plasmas* **7**, 2340 (2000).
[10] D. L. Eggleston, C. F. Driscoll, B. R. Beck, A. W. Hyatt, and J. H. Malmberg, *Phys. Fluids* **B4**, 3432 (1992).
[11] C. F. Driscoll and J. H. Malmberg, *Phys. Rev. Lett.* **50**, 167 (1983).
[12] D. L. Eggleston, *Phys. Plasmas* **4**, 1196 (1997).
[13] J. M. Kriesel and C. F. Driscoll, *Phys. Rev. Lett.* **85**, 2510 (2000).